

Analysis of blood flow through curved artery with mild stenosis

Kafle J.¹, Gaire H. P.¹, Pokhrel P. R.², Kattel P.^{3,*}

¹Central Department of Mathematics, Tribhuvan University, Kirtipur, Kathmandu, Nepal

²Department of Mathematics, R R Campus, Tribhuvan University, Kathmandu, Nepal

³Department of Mathematics, Tri-Chandra Multiple Campus, Tribhuvan University, Kathmandu, Nepal,

*Corresponding author: pkattel526@gmail.com

(Received 9 June 2021; Accepted 21 January 2022)

Building-up of plaque narrows arteries, decreasing blood flow to the heart, causing chest pain, shortness of breath, or other coronary artery disease signs and symptoms. Implementing Navier–Stokes equations in a cylindrical coordinate system and assuming axial symmetry under laminar flow conditions, the study has been conducted on the two aspects of blood flow dynamics viz., velocity profile and volumetric flow rate of blood around curved stenosis with a variation of curvature of the artery and the stenosis thickness. The blood flow behavior taking different values for the viscosity coefficient has been also studied.

Keywords: *arterial stenosis, blood viscosity, blood flow curvature effect, velocity profile, volumetric flow rate.*

2010 MSC: 76Z05, 92C35

DOI: 10.23939/mmc2022.02.217

1. Introduction

Stenosis in an artery generally occurs due to the accumulation of cholesterol-laden plaque in its walls resulting in a narrowing of the passage of blood as well as a loss of elasticity that leads to stroke and heart attack. In the regions where the blood flow is disturbed and at low wall shear stress, narrowing of the lumen may occur. Enhanced flow disturbances are established once plaque develops and encroaches the lumen [1]. One of the major causes of human deaths worldwide is the cardiovascular disease: ischemia, atherosclerosis, and angina pectoris. Stroke is the second most common cause of death that follows heart disease. The major cause of stroke is the blockage of blood vessels or plaque rupture [2, 3].

Some researchers studied the blood flow characteristics considering it as a Newtonian fluid flowing at a high shear rate through an artery of large diameter with mild stenosis [2, 4–6]. Padmanabhan and Jayaraman [7] obtained an analytical solution to a mathematically modeled problem of blood flow in a curved stenosed artery by using system of toroidal coordinate and perturbation theory. They discussed the impedance and shear stress in the wall and observed in a uniform curved tube the point of maximum shear changes over from the inner bend to the outer bend. Moreover, stenotic surface provides an additional curvature and the point of maximum shear varies with the cross section. The effect of stenosis was such that most of the flow characteristics depend on the axial distance and the secondary streamlines at every cross section become different. Chakravarty [8] observed that blood as a suspension behaves like a non-Newtonian fluid at low shear rates in relatively smaller arteries. Although stenotic deposits are in irregular shapes, cosine-type or smooth regular shapes are generally found to be considered in three-dimensional modeling of blood flow in arteries.

Dash et al. [9] derived an approximate analytic solution to the problem of blood flow through a small curvature catheterized artery in mild stenosis with a double series perturbation analysis. They observed the effect of stenosis on the flow to be dominant over that of the curvature. When a catheter was inserted into an artery, it brought a considerable change in the flow pattern. Due to the catheter,

the secondary streamlines divided each half of the cross-sectional plane into two parts forming two loops. They also observed that, in the presence of curvature and stenosis, and depending on the value of catheter size ranging from 0.1 mm to 0.4 mm, the pressure drop increased by a factor ranging from 1.6 to 5.16 for the Reynolds number, $Re = 50$ and from 1.56 to 5.03 for $Re = 10$ for some appropriately chosen parameters. Schilt et al. [10] performed some experiments to reveal the effect of time varying curvature on flow velocity profile in a curved tube model of coronary arteries. They devised an in vitro flow model consisted of a flexible curved tube through which fluid flow under steady imposed pressure gradient. The dynamic curvature was given by the varying radius of curvature of the tube using stepper motor and carriage. In their experiments, the skewing of the axial velocity profile depended on the instantaneous dynamic vessel movement. The greater skewing occurred when carriage moved obliquely to the main direction of flow than when the carriage moved perpendicularly. Depending upon the actual movement of the tube, the velocity profile along the axis was found to be more or less skewed toward the outer wall.

Nosovitsky et al. [11] used computational fluid dynamic techniques to determine the distribution of velocity and wall shear stress (WSS) in both steady and phasic-flow models of a curved coronary artery with different degrees of stenosis. They observed, without stenosis and with 25% stenosis, that WSS and velocity became higher at the outer wall than at the inner wall. For higher degree of stenosis, laminar flow separation occurred, and inner wall exposed to shear stress that both spatially and temporally varied in a great deal. Santamarina et al. [12] studied the flow of blood through curved tube with time variant radius of curvature. They observed that the overall behavior of flow entering a curved tube with dynamically varying curvature was not much different from that of a static curved tube. The velocity profile were skewed towards the inner wall of curvature, although two tube diameters of the velocity profile were skewed toward the outer wall and a secondary velocity was established.

Yao et al. [13] developed a computational model of three-dimensional blood flow in curved arteries with elliptic stenosis. The study also demonstrated the significant appearance of secondary flow. Furthermore, the secondary flow in a curved artery was found to bring about elevated shear stress on the vessel wall. Moreover, high WSS, high velocity skewing and secondary flow for stenosis occurred at a curved section. So, even a mild stenosis that occurs at high curved section can produce worse effects than a more acute stenosis that occurred on a straight artery. Liu [14] studied the influence of stenosis on the pulsatile blood flow pattern in curved arteries with stenosis at inner wall using computer simulations. The results demonstrated that when the severity of a stenosis at the inner wall of a curved artery reached a certain level, the flow pattern in the downstream of the artery showed a dramatic change as compared to that of a curved artery with no stenosis. The work reported an analysis of a flow separation area at the inner wall of the post stenosis region in curved arteries with a stenosis. They also found that the secondary flow becomes stronger and the pattern varies irregularly in the downstream curved stenotic arteries due to the presence of a stenosis. The distribution of the velocity fields in the curvature plane and the negative axial velocity revealed the separation of the flow at the inner wall of the post-stenosis region and at the outer wall in the middle of downstream.

Mathematical methods and modeling techniques find their ample applications in different branches of science, such as geophysics [15–18], environment [19], physics [20, 21], electronics [22], in particular, in mathematical biology, especially in the study of epidemiology and body fluid [2, 5, 6, 23–25]. In this contribution, we study the blood flow dynamics by analyzing the velocity and volumetric flow rate of blood through a curved artery with mild stenosis incorporating the curvature as proposed in. In physics and engineering, and in particular, in fluid dynamics, the volumetric flow rate (also known as volume flow rate, rate of fluid flow, or volume velocity) is the volume of fluid which passes per unit time; usually it is represented by the symbol Q . The SI unit is cubic meter per second ($\text{m}^3 \text{s}^{-1}$) [5]. $\lambda\kappa$ is dynamic curvature and μ is the coefficient of viscosity. Units of $\lambda\kappa$ and μ are $\text{mm}^{-1} \text{s}$ and $\text{gram mm}^{-1} \text{s}^{-1}$ respectively.

2. Methods

When there is no stenosis or there is a pair of axi-symmetric stenosis, the motion is assumed to be symmetrical about the axis of z in a cylindrical polar coordinates (r, θ, z) . Let the three velocity components and pressure of the blood at the point (x, y, z) with Cartesian spatial coordinates at time t in a cylindrical artery be $u(x, y, z, t)$, $v(x, y, z, t)$, $w(x, y, z, t)$ and $p(x, y, z, t)$ respectively. The continuity equation in differential form assuming constant density and steady-state flow is [4]:

$$\frac{\partial u}{\partial x} + \frac{\partial v}{\partial y} + \frac{\partial w}{\partial z} = 0. \tag{1}$$

The continuity equation in cylindrical coordinate system is in the form [5]:

$$\frac{1}{r} \frac{\partial}{\partial r}(rv^r) + \frac{\partial}{\partial z}(v^z) = 0, \tag{2}$$

where v^r is the radial velocity, v^z is the velocity along z -direction; the equation assumes that the angular velocity $v^\theta = 0$. The Navier–Stokes (N-S) equations of motion in cylindrical coordinate system are given by [5]:

$$\rho \left(\frac{\partial v^r}{\partial t} + v^r \frac{\partial v^r}{\partial r} + v^z \frac{\partial v^r}{\partial z} \right) = -\frac{\partial p}{\partial r} + \mu \left(\frac{\partial^2 v^r}{\partial r^2} + \frac{\partial^2 v^r}{\partial z^2} + \frac{1}{r} \frac{\partial v^r}{\partial r} - \frac{v^r}{r^2} \right), \tag{3}$$

$$\rho \left(\frac{\partial v^z}{\partial t} + v^r \frac{\partial v^z}{\partial r} + v^z \frac{\partial v^z}{\partial z} \right) = -\frac{\partial p}{\partial z} + \mu \left(\frac{\partial^2 v^z}{\partial r^2} + \frac{\partial^2 v^z}{\partial z^2} + \frac{1}{r} \frac{\partial v^z}{\partial r} \right). \tag{4}$$

Due to axi-symmetric flow, $v^\theta = 0$, and v^r, v^z and p are also independent of θ . The viscosity μ and density ρ of the blood are both assumed to be constants. Considering steady flow, the velocity component parallel to the axis, $v^r = 0$. So, we consider $v^z = v$. Now, the equations (2)–(4) give

$$-P(z) \frac{r}{\mu} = \frac{\partial}{\partial r} \left(r \frac{\partial v}{\partial r} \right), \tag{5}$$

where $P(z) = -\frac{\partial p}{\partial z}$. With the boundary condition as

$$\begin{aligned} v &= 0 \quad \text{at} \quad r = R(z), \quad \text{for} \quad -z_0 \leq z \leq z_0, \\ v &= 0 \quad \text{at} \quad r = R_0, \quad \text{for} \quad |z| \geq z_0, \end{aligned} \tag{6}$$

and the shape function $R(z)$ for the radial structure of the surface of cylindrical pipe as shown in Fig. 1 is given by the cosine function [5]:

$$\frac{R}{R_0} = 1 - \frac{\delta}{2R_0} \left(1 + \cos \frac{\pi z}{z_0} \right). \tag{7}$$

Integrating (5) with respect to r taking z as constant, and employing the boundary condition (6), we get

$$v = \frac{P}{4\mu} (R^2 - r^2). \tag{8}$$

This shows that the velocity is maximum along the axis and zero at the surface of the artery. As v is a function of r and z , the volumetric flow rate through the cylindrical tube can be found as [18]:

$$Q = \frac{\pi P(z)}{8\mu} R^4(z).$$

Since Q is independent of z , this equation gives $P(z)$ as a function of z . This shows that pressure gradient varies inversely as the fourth power of the surface distance of the stenosis from the axis of the artery, and thus pressure gradient is minimum at the middle and maximum at the ends of the stenosis.

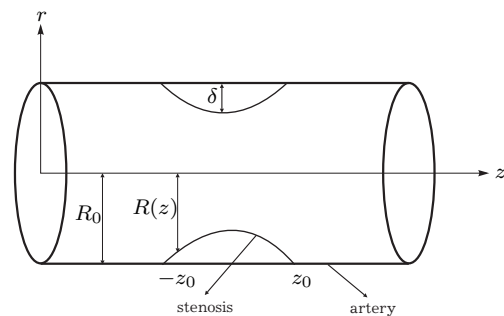


Fig. 1. Sketch of a section of a cylindrical artery with stenosis.

2.1. Velocity of blood flow in curvature model

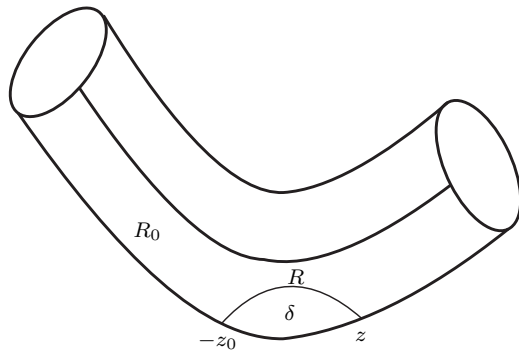


Fig. 2. Sketch of a section of a curved cylindrical artery with stenosis.

In Pokhrel et al. [6], the proposed curvature model is:

$$-P(z) = \frac{\mu}{r} \frac{\partial}{\partial r} \left(r \frac{\partial v}{\partial r} + \lambda \kappa v^2 \right), \quad (9)$$

where $\lambda \kappa$ is the dynamic curvature of artery with stenosis as in Fig.2. So, the equation (9) can be arranged as:

$$-P(z) \frac{r}{\mu} = \frac{\partial}{\partial r} \left(r \frac{\partial v}{\partial r} + \lambda \kappa v^2 \right). \quad (10)$$

Equation (10) is integrated with respect to r to obtain

$$-P(z) \frac{r^2}{2\mu} + D(z) = r \frac{\partial v}{\partial r} + \lambda \kappa v^2, \quad (11)$$

where $D(z)$ is the constant of integration with respect to r . Applying the boundary conditions as $\partial v / \partial r = 0$, and $v = PR^2 / 4\mu$ at $r = 0$ along z -axis in (11) yields

$$D(z) = \lambda \kappa \frac{P^2}{16\mu^2} R^4.$$

Substituting this expression for $D(z)$ in (11) and using v from (8), we get

$$\frac{\partial v}{\partial r} = -\frac{Pr}{2\mu} + \frac{\lambda \kappa P^2 R^2 r}{8\mu^2} - \frac{\lambda \kappa P^2 r^3}{16\mu^2}.$$

Integrating it with respect to r gives

$$v(r) = -\frac{Pr^2}{4\mu} + \frac{\lambda \kappa P^2 R^2 r^2}{16\mu^2} - \frac{\lambda \kappa P^2 r^4}{64\mu^2} + E(z), \quad (12)$$

where $E(z)$ is a constant of integration. Now the boundary condition $v = 0$ at $r = R$ gives

$$E(z) = \frac{PR^2}{4\mu} - \frac{3}{64} \frac{\lambda \kappa P^2 R^4}{\mu^2}.$$

Substituting this expression for $E(z)$ in (12) gives

$$v(r) = \frac{P}{4\mu} (R^2 - r^2) + \frac{\lambda \kappa P^2}{16\mu^2} \left[R^2 r^2 - \frac{r^4}{4} - \frac{3}{4} R^4 \right]. \quad (13)$$

This is the expression for the velocity distribution function for blood flow in a curved artery.

2.2. Velocity at the surface and on the axis

At the surface of the artery, $r = R$. Then, from (13), the velocity on the surface is zero, i.e., $v(R) = 0$ as shown in Fig. 3. On contrary, for $r = 0$ (i.e., on the z -axis), (13) gives the maximum velocity:

$$v = v_{max} = \frac{PR^2}{4\mu} - \frac{3\lambda \kappa P^2}{64\mu^2} R^4.$$

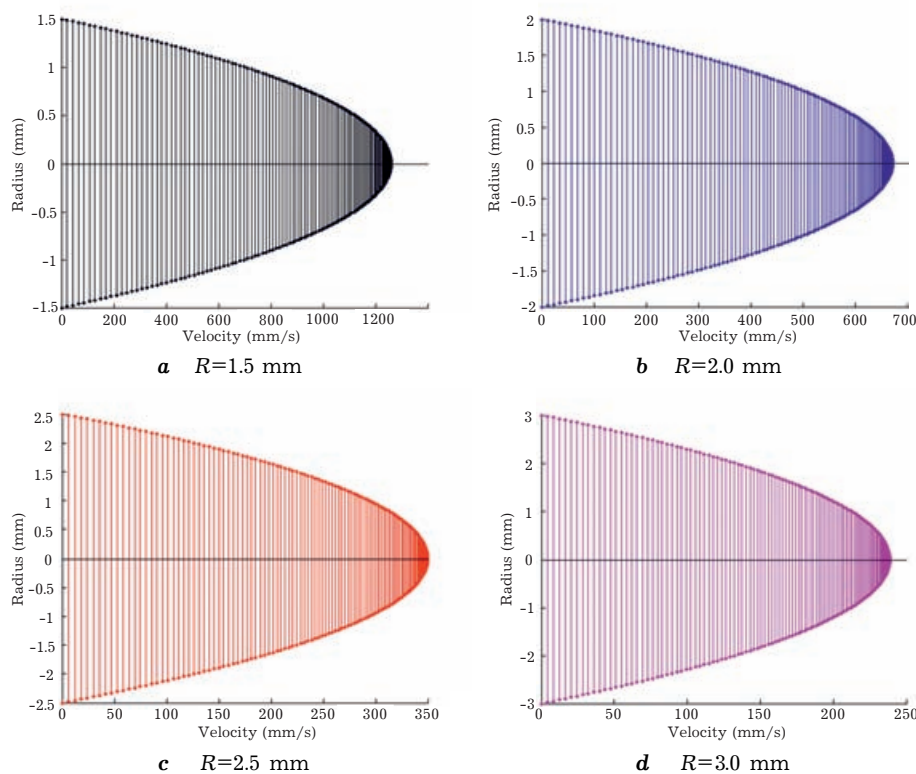


Fig. 3. Velocity profile of blood in artery with mild stenosis of different radius for zero curvature ($\lambda\kappa = 0 \text{ mm}^{-1} \text{ s}$).

2.3. Volumetric flow rate in curved artery

The volumetric flow rate through the curved artery is:

$$Q = \int_0^{R(z)} 2\pi r v \, dr = \frac{\pi P}{8\mu} R^4 - \frac{\pi \lambda \kappa P^2}{8\mu^2} \frac{R^6}{6}. \tag{14}$$

When there is no curvature (i.e., $\lambda\kappa = 0$), then the expression for the volumetric flow rate becomes

$$Q = \frac{\pi P}{8\mu} R^4, \tag{15}$$

which is reduced to that discussed in Pokhrel et al. [6].

3. Results and discussion

This section includes simulation results and discussion on velocity and volumetric flow rate of blood.

3.1. Velocity profile of blood flow through a stenotic artery without curvature

Velocity profile exhibits the magnitude of velocity and characteristics of the flow like direction. Figure 3 shows the velocity profiles of blood on coronary artery with different radii of stenosis in case there is no curvature (i.e., $\lambda\kappa = 0$). Pressure gradient is initially taken to be 20.15 mm of Hg [5]. Since pressure gradient acting on a fluid body will accelerate the fluid, it is a dynamic force field while computing velocity profiles and volumetric flow rates.

For different radius R of stenosis, the coefficient of viscosity is also different. As R decreases, μ decreases, and as R increases, μ increases [5]. μ takes the value of 0.19, 0.09, 0.03 and 0.009 $\text{gm mm}^{-1} \text{ s}^{-1}$ for $R = 3, 2.5, 2$ and 1.5 mm respectively. The velocity profile diagram shows that as the height δ of stenosis increases (i.e., effective radius of artery R decreases), the blood flow velocity increases. In a

stream-line flow of a liquid, according to equation of continuity, av is always constant, where a is the area of cross-section and v is the velocity of the fluid flow. When blood flowing in larger cross section enters into narrower cross section, the velocity of fluid increases. The values of R differ for Fig. 3 and are constant for Figs. 4–7, where ‘ r ’ is the radii variable in (13). Although δ is not used in our computations directly, R and δ are complementary to each other. When δ increases, R decreases, and vice versa. The maximum velocity is 1260 mm/s (126 cm/s) with $R = 1.5$ mm and the least velocity is of 238 mm/s (23.8 cm/s) for $R = 3$ mm. It is evident that velocity is maximum along the axis and zero on the wall. The model simply allows us to sketch velocity profile and volumetric flow rates at different curvature of artery for designated stenotic radii.

3.2. Velocity profile on stenosis with curvature

Figure 4 depicts the velocity profiles for different curvature of artery with stenosis of 3 mm radii.

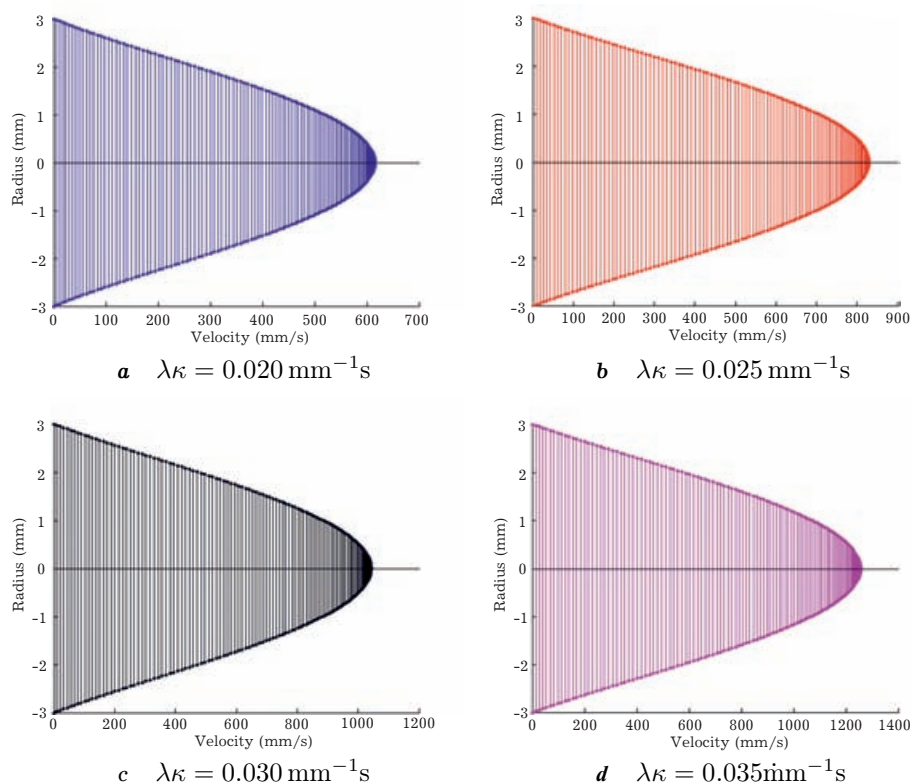


Fig. 4. Velocity profile of blood flow in artery with mild stenosis with arterial radius 3 mm for different curvature.

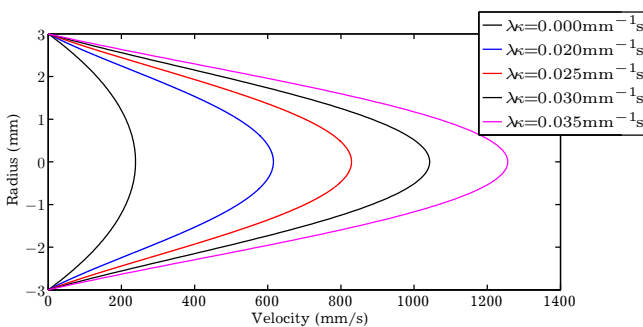


Fig. 5. Velocity profile for different values of $\lambda\kappa$.

Since we are considering the artery on outer wall of the heart (pulmonary artery), the curvature becomes dynamic and changes with time. The velocity profile shows that as the curvature $\lambda\kappa$ of artery gradually increases, the blood flow velocity also increases. The maximum velocity is 1250 mm/s (125 cm/s) in the largest curvature of artery ($\lambda\kappa = 0.035 \text{ mm}^{-1} \text{ s}$) and the least velocity is 620 mm/s (62 cm/s) with the smallest curvature ($\lambda\kappa = 0.02 \text{ mm}^{-1} \text{ s}$). Velocity is again maximum along the axis and zero on the wall. The observation of velocity profiles on a 3 mm

radius stenosis is for two cases: no-curvature ($\lambda\kappa = 0 \text{ mm}^{-1} \text{ s}$) and different degrees of curvature ($\lambda\kappa = 0.02, 0.025, 0.03, 0.035 \text{ mm}^{-1} \text{ s}$) is evident in Fig. 5. Centripetal acceleration is inversely proportional to the radius of curvature and directly proportional to the curvature. Higher the curvature, more will be the centripetal acceleration, faster will be the fluid flow. So blood flow in case of zero curvature ($\lambda\kappa = 0 \text{ mm}^{-1} \text{ s}$) is least and of the highest curvature ($\lambda\kappa = 0.035 \text{ mm}^{-1} \text{ s}$) is highest.

3.3. Volumetric rate of blood flow on stenosis without curvature

Figure 6 illustrates that the volumetric flow rate of blood in a normal artery ($\lambda\kappa = 0$) with mild stenosis for different values of coefficient of viscosity μ . As R decreases, μ decreases, and as R increases, μ increases [4]. For the least value of $\mu = 0.035 \text{ gram mm}^{-1} \text{ s}^{-1}$, the flow rate is highest and for the maximal value of $\mu = 0.33 \text{ gram mm}^{-1} \text{ s}^{-1}$, the flow rate is least. Less viscous the fluid becomes, more rapidly it can flow. Mean flow rate is $9124 \text{ mm}^3/\text{s}$ ($\approx 9.124 \text{ ml/s}$). As more the stenosis widens, the effect of μ is evident. Larger the values of μ , less steeper the curves become. But for narrower artery due to stenosis, the effects of μ tend to diminish and curves come closer and closer. When R reduces to zero, the artery is absolutely blocked due to stenosis, and there is no flow at all.

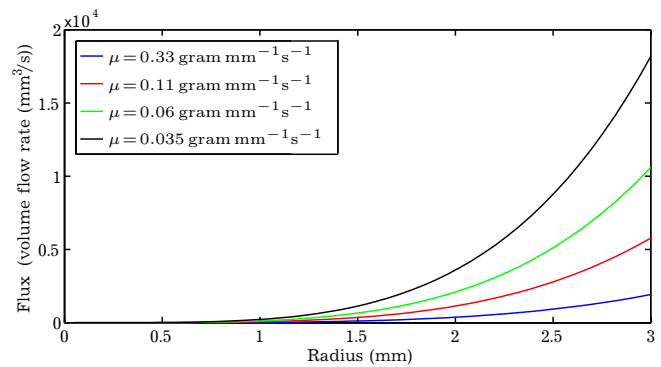


Fig. 6. Volumetric flow rate coefficient of viscosity μ for zero curvature ($\lambda\kappa = 0 \text{ mm}^{-1} \text{ s}$).

3.4. Volumetric flow rate on stenosis with curvature

Figure 7 depicts the volumetric flow rate of blood in a curved artery with mild stenosis for different values of curvature $\lambda\kappa$ and fixed value of coefficient of viscosity $\mu = 0.06 \text{ gram mm}^{-1} \text{ s}^{-1}$. The velocity profile for curved artery shows that more is the curvature, higher will be the velocity. For least value of $\lambda\kappa = 0.02 \text{ mm}^{-1} \text{ s}$, the flow rate is least and for greatest value of $\lambda\kappa = 0.035 \text{ mm}^{-1} \text{ s}$, the flow rate is maximum. Mean flow rate is $135182 \text{ mm}^3/\text{s}$ ($\approx 135.182207 \text{ ml/s}$). As more the stenosis widens, the effect of $\lambda\kappa$ is evident. More is the value of $\lambda\kappa$, more steeper will be the curve. But for narrower stenosis, the effect of $\lambda\kappa$ diminishes and the curve comes closer and closer. The artery is absolutely blocked at $R = 0$ and there is no flow at all. The observation of volumetric flow rates on a 3 mm radius stenotic artery for two cases: no-curvature ($\lambda\kappa = 0 \text{ mm}^{-1} \text{ s}$) and different degrees of curvature ($\lambda\kappa = 0.02, 0.025, 0.03, 0.035 \text{ mm}^{-1} \text{ s}$) are evident. The coefficient of viscosity is assumed to be constant ($\mu = 0.06 \text{ gram mm}^{-1} \text{ s}^{-1}$) in all cases. Centripetal acceleration is inversely proportional to the radius of curvature and directly proportional to the curvature. Higher the curvature, more will be the centripetal acceleration, faster the fluid flow and faster will be the flow discharge. Thus, volumetric flow rate in case of zero curvature ($\lambda\kappa = 0 \text{ mm}^{-1} \text{ s}$) is least and of peak curvature ($\lambda\kappa = 0.035 \text{ mm}^{-1} \text{ s}$) is maximum.

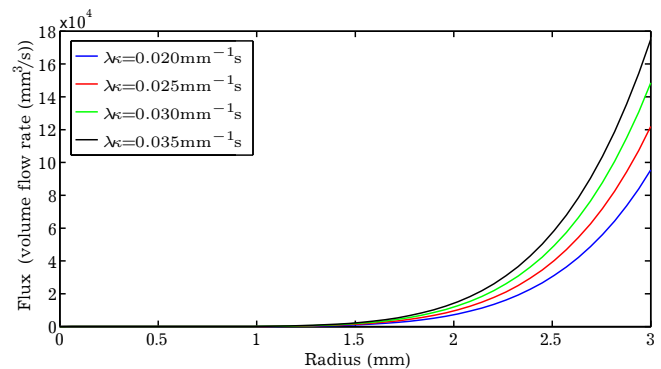


Fig. 7. Volumetric flow rate for different $\lambda\kappa$ values in curved artery ($\mu = 0.06 \text{ gram mm}^{-1} \text{ s}^{-1}$).

4. Conclusions

We have presented the model for blood flow in a mildly stenosed artery with curvature. We have used the boundary conditions to find the velocity distribution on the surface and along the direction of the z -axis. We compared the velocity distribution on the cylindrical-shaped curved artery with and without curvatures. We computed and analyzed the volumetric rate of blood flow on the curved artery with mild stenosis with curvature. We also compared the results with and without curvature on an artery. The present mathematical modeling of blood flow in a stenosed artery with the combined effect of curvature and viscosity unveils the peculiar properties of blood flow dynamics. There is a significant effect of curvature on the blood flow velocity and volumetric flow rate. It is observed that in the absence of curvature and depending on the effective radii of the artery due to stenosis ranging from 1.5 mm to 3 mm, the flow velocity decreases from 1260 mm/s to 238 mm/s. With the fixed 3 mm radius of stenosis and increasing factor of curvature from $0.02 \text{ mm}^{-1} \text{ s}$ to $0.035 \text{ mm}^{-1} \text{ s}$, the flow velocity increases from 620 mm/s to 1250 mm/s. Meanwhile, for an artery with stenosis of 3 mm effective radius depending on the factor of coefficient of viscosity μ ranging from $0.035 \text{ gram mm}^{-1} \text{ s}^{-1}$ to $0.33 \text{ gram mm}^{-1} \text{ s}^{-1}$, the flow rate decreases from $1.814 \times 10^4 \text{ mm}^3/\text{s}$ to $1912 \text{ mm}^3/\text{s}$ and for the factor of curvature $\lambda\kappa$ ranging from $0.02 \text{ mm}^{-1} \text{ s}$ to $0.035 \text{ mm}^{-1} \text{ s}$, the flow rate increases from $9.521 \times 10^4 \text{ mm}^3/\text{s}$ to $1.745 \times 10^5 \text{ mm}^3/\text{s}$.

Acknowledgment

Hari Parsad Gaire acknowledges National Youth Council, Sanothimi, Bhaktapur, Nepal for providing financial support as a master thesis grant.

-
- [1] Tan F. P. P., Soloperto G., Wood N. B., Thom S., Hughes A., Xu X. Y. Advanced computational models for disturbed and turbulent flow in stenosed human carotid artery bifurcation. *Proceeding of the 4th Kuala Lumpur International Conference on Biomedical Engineering 2008*. **21**, 390–394 (2008).
 - [2] Phaijoo G. R. Mathematical study of blood flow characteristics during catheterization in stenosed artery. Unpublished dissertation in partial fulfillment of the requirements of Master of Philosophy, School of Science, Kathmandu University, Nepal (2013).
 - [3] Pralhad J. N., Schultz D. H. Modeling of arterial stenosis and its applications to blood diseases. *Mathematical Biosciences*. **190** (2), 203–220 (2004).
 - [4] Jain M., Sharma G. C., Singh R. Mathematical modeling of blood flow in a stenosed artery under MHD effect through porous medium. *International Journal of Engineering*. **23** (3), 243–252 (2010).
 - [5] Kapur J. N. Mathematical models in biology and medicine. In: *Models for blood flows*. Affiliated East-West Press Pvt. Ltd. **347** (1985).
 - [6] Pokhrel P. R., Kafle J., Kattel P., Gaire H. P. Analysis of blood flow through artery with mild stenosis. *Journal of Institute of Science and Technology*. **25** (2), 33–38 (2020).
 - [7] Padmanabhan N., Jayaraman G. Flow in a curved tube with constriction — an application to the arterial system. *Medical and Biological Engineering and Computing*. **22** (3), 216–224 (1984).
 - [8] Chakravarty S. Effects of stenosis on the flow-behaviour of blood in an artery. *International Journal of Engineering Science*. **25** (8), 1003–1016 (1987).
 - [9] Dash R. K., Jayaraman G., Meheta K. N. Flow in a catheterized curved artery with stenosis. *Journal of Biomechanics*. **32** (1), 49–61 (1999).
 - [10] Schilt S., Moore J. E., Delfino A., Meister J. J. The effects of time-varying curvature on velocity profiles in a model of the coronary arteries. *Journal of Biomechanics*. **29** (4), 469–474 (1996).
 - [11] Nosovitsky V. A., Ilegbusi O. J., Jiang J., Stone P. H., Feldman C. L. Effects of curvature and stenosis-like narrowing on wall shear stress in a coronary artery model with phasic flow. *Computers and Biomedical Research*. **30**, 61–82 (1997).
 - [12] Santamarina A., Weydahl E., Siegel J. M., Moore J. E. Jr. Computational analysis of flow in a curved tube model of the coronary arteries: Effects of time-varying curvature. *Annals of Biomedical Engineering*. **26**, 944–954 (1998).

- [13] Yao H., Ang K. C., Yeo J. H., Sim E. K. W. Computational modelling of blood flow through curved stenosed arteries. *Journal of Medical Engineering & Technology*. **24** (4), 163–168 (2000).
- [14] Liu B. The influences of stenosis on the downstream flow pattern in curved arteries. *Medical Engineering & Physics*. **29** (8), 868–876 (2007).
- [15] Kafle J., Pokhrel P. R., Khattri K. B., Kattel P., Tuladhar B. M., Pudasaini S. P. Submarine landslide and particle transport in mountain lakes, reservoirs and hydraulic plants. *Annals of Glaciology*. **57** (71), 232–244 (2016).
- [16] Kafle J., Kattel P., Mergili M., Fischer J.-T., Pudasaini S. P. Dynamic response of submarine obstacles to two-phase landslide and tsunami impact on reservoirs. *Acta Mechanica*. **230** (9), 3143–3169 (2019).
- [17] Kattel P., Khattri K. B., Pokhrel P. R., Kafle J., Tuladhar B. M., Pudasaini S. P. Simulating glacial lake outburst floods with a two-phase mass flow model. *Annals of Glaciology*. **57** (71), 349–358 (2016).
- [18] Kattel P., Kafle J., Fischer J.-T., Mergili M., Tuladhar B. M., Pudasaini S. P. Interaction of two-phase debris flow with obstacles. *Engineering Geology*. **242**, 197–217 (2018).
- [19] Paudel K., Bhandari P., Kafle J. Analytical solution for advection-dispersion equation of the pollutant concentration using laplace transformation. *Journal of Nepal Mathematical Society*. **4** (1), 33–40 (2021).
- [20] Kafle J., Bagale L., K. C. D. J. Numerical solution of parabolic partial differential equation by using finite difference method. *Journal of Nepal Physical Society*. **6** (2), 57–65 (2020).
- [21] Pokhrel P. R., Lamsal B., Kafle J., Kattel P. Analysis of displacement of vibrating of mass-spring due to opposition force. *Tribhuvan University Journal*. **35** (1), 21–32 (2020).
- [22] Kafle J., Thakur B. K., Bhandari I. B. Visualization formulation and intuitive explanation of iterative methods for transient analysis of series RLC circuit. *Bibechana*. **18** (2), 9–17 (2021).
- [23] Adhikari K., Gautam R., Pokhrel A., Uprety K. N., Vaidya N. K. Transmission dynamics of COVID-19 in Nepal: Mathematical model uncovering effective controls. *Journal of Theoretical Biology*. **521** (21), 110680 (2021).
- [24] Agarwal P., Nieto J. J., Ruzhansky M., Torres D. F. M. Analysis of infectious disease problems (Covid-19) and their global impact. Springer, Singapore (2021).
- [25] Shrestha S., Gurung D. B., Gokul K. C. Mathematical modeling of temperature variation in breast tissue with and without tumor/cyst during menstrual cycle. *Mathematical Modeling and Computing*. **8** (2), 192–202 (2021).

Аналіз кровотоку через викривлену артерію з легким стенозом

Кафле Дж.¹, Гайре Х. П.¹, Похрел П. Р.², Каттель П.³

¹Центральна кафедра математики, Університет Трібхуван, Кіртіпур, Катманду, Непал

²Кафедра математики, Кампус RR, Університет Трібхуван, Катманду, Непал

³Кафедра математики, Багатoproфільний кампус Трі-Чандра, Університет Трібхуван, Катманду, Непал

Утворення бляшок звужує артерії, зменшуючи приплив крові до серця, викликаючи біль у грудях, задишку або інші ознаки та симптоми ішемічної хвороби серця. Реалізуючи рівняння Нав'є—Стокса в циліндричній системі координат і припускаючи осьову симетрію потоку за умов ламінарного потоку, проведено дослідження двох аспектів динаміки кровотоку, а саме: профілю швидкості та об'ємної швидкості кровотоку навколо викривленого стенозу зі зміною кривизни артерії та товщини стенозу. Також досліджено поведінку кровотоку для різних значень коефіцієнта в'язкості.

Ключові слова: стеноз артерій, в'язкість крові, вплив кривизни на кровотік, профіль швидкості, об'ємна швидкість потоку.